Virology 475 (2015) 129–138

Contents lists available at ScienceDirect

Virology

journal homepage: www.elsevier.com/locate/yviro

Attenuation of monkeypox virus by deletion of genomic regions

Juan G. Lopera [a,*], Elizabeth A. Falendysz [b], Tonie E. Rocke [b], Jorge E. Osorio [a,**]

[a] Department of Pathobiological Sciences, School of Veterinary Medicine, University of Wisconsin, Madison, WI, USA
[b] National Wildlife Health Center, U.S. Geological Survey, Madison, WI, USA

ARTICLE INFO

Article history:
Received 11 September 2014
Returned to author for revisions
20 October 2014
Accepted 3 November 2014
Available online 1 December 2014

Keywords:
Monkeypox virus
Variola virus
Vaccinia virus
Monkeypox virus pathogenesis
Virulence factors
Viral replication
In vivo bioluminescence imaging

ABSTRACT

Monkeypox virus (MPXV) is an emerging pathogen from Africa that causes disease similar to smallpox. Two clades with different geographic distributions and virulence have been described. Here, we utilized bioinformatic tools to identify genomic regions in MPXV containing multiple virulence genes and explored their roles in pathogenicity; two selected regions were then deleted singularly or in combination. *In vitro* and *in vivo* studies indicated that these regions play a significant role in MPXV replication, tissue spread, and mortality in mice. Interestingly, while deletion of either region led to decreased virulence in mice, one region had no effect on *in vitro* replication. Deletion of both regions simultaneously also reduced cell culture replication and significantly increased the attenuation *in vivo* over either single deletion. Attenuated MPXV with genomic deletions present a safe and efficacious tool in the study of MPX pathogenesis and in the identification of genetic factors associated with virulence.

Introduction

Monkeypox virus (MPXV; *Poxviridae*, *Orthopoxvirus*) causes human monkeypox (MPX), a disease with a clinical presentation that resembles human smallpox (Cann et al., 2013; Huhn et al., 2005). Human MPX is endemic in equatorial Africa, and no specific wild animal reservoir has been identified. Recent epidemiologic studies have shown an increase in human MPX cases in the last 30 years in the central region of Africa (Reynolds and Damon, 2012; Rimoin et al., 2010). In 2003, the virus was introduced to the United States through the importation of infected rodents from West Africa (Likos et al., 2005; Reynolds and Damon, 2012). In 2005, human MPX cases were identified in southern Sudan (now South Sudan), and are thought to be associated with translocations of infected humans or animals from Central Africa (Nakazawa et al., 2013).

The emergence of MPXV, as well as its potential threat as a bioterrorism weapon, warrants the study of its mechanisms of infection, virulence factors, and pathogenesis (Breman and Henderson, 1998; Reynolds and Damon, 2012; Rimoin et al., 2010). Genomic comparisons of MPXV human isolates have revealed the existence of two highly diverse clades of MPXV with different geographic distribution and pathogenicity. Infections with MPXVs isolated from Central Africa (MPXV/Congo) cause more severe disease in humans and rodents compared to viruses in the West African clade (MPXV/USA) (Chen et al., 2005; Hutson and Damon, 2010; Likos et al., 2005). Comparisons between these MPXV clades and related orthopoxvirus (OPXV) genomes have shown that although these are closely related viruses, they contain several highly variable genomic regions (termed here regions [R]) that are characterized by high mutation rates, insertions, deletions, and gene truncations (Chen et al., 2005; Hendrickson et al., 2010; Shchelkunov et al., 2001). In MPXV and other OPXVs these regions contain several known host range and immunomodulatory (IMM) genes (Seet et al., 2003). These genes have evolved specifically to simultaneously inhibit diverse processes such as pattern-recognition receptor signaling, apoptosis, chemokine and cytokine function, and lymphocyte and antibody activity (Fernandez de Marco Mdel et al., 2010; Hammarlund et al., 2008; Kindrachuk et al., 2012; Weaver and Isaacs, 2008). Whereas previous evaluations of MPXV virulence factors have predominantly focused on the function and characterization of individual viral genes, these studies demonstrated that individual genes were not solely responsible for the observed differences in pathogenicity between MPXV clades (Estep et al., 2011; Hudson et al., 2012). In contrast, we evaluated the effect of deletions of large genomic regions in MPXV that contain several host range and IMM genes to facilitate selection of candidate virulence factors involved in pathogenesis. Specifically, we quantified and compared the effect of deletion of two genomic regions in a Central African MPXV-Congo strain. The impacts of these deletions on replication

* Corresponding author. Tel.: +1 608 890 0480; fax: +1 608 262 7420.
** Corresponding author. Tel.: +1 608 890 0252.
E-mail addresses: loperapena@wisc.edu (J.G. Lopera), osorio@svm.vetmed.wisc.edu (J.E. Osorio).

http://dx.doi.org/10.1016/j.virol.2014.11.009
0042-6822/

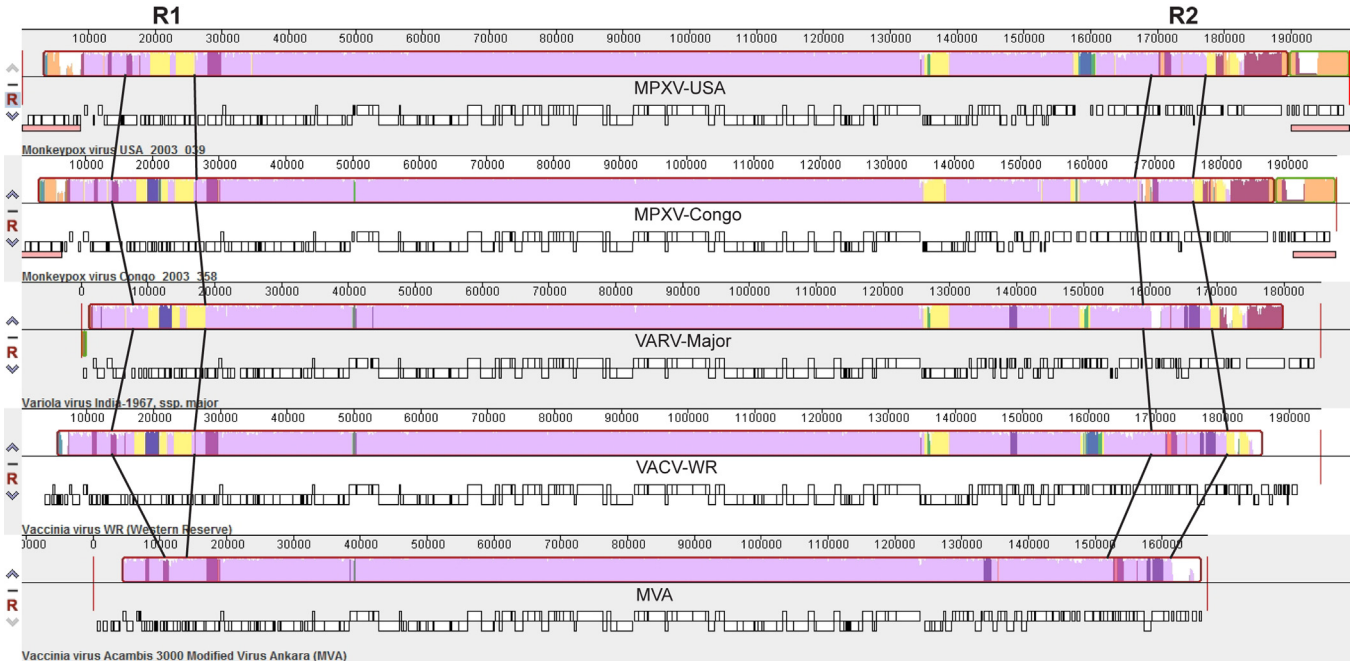

Fig. 1. Sequence comparisons and identification of target genomic regions. The colored bars inside the genomic blocks represent the level of sequence similarities between viruses. Regions with high sequence similarity are shown in light purple. Regions with mutations, insertions, and deletions of genes are represented in colored bars. White bars represent genomic sequences present in only one viral genome. Boxes surround predicted genomic regions in MPXV clades. Lines link orthologous genomic regions in MPXV, variola virus (VARV), vaccinia virus (VACV) and modified vaccinia ankara (MVA) genomes. Genomic regions were selected based upon sequence analysis utilizing MAUVE and DAMBE software. Regions characterized in this study are indicated by R1 and R2.

kinetics, host immune response, host tissue tropism and virulence were analyzed using cell culture, immunoassays and *in vivo* imaging. The research described herein identified regions in the MPXV genome that can inform the selection of candidate genes for future study to more fully dissect the molecular determinants of virulence in MPXV.

Results

Identification of genomic regions and generation of recombinant viruses

Genomic alignments and sequence comparisons between MPXV clades and other related OPXV helped to identify two target genomic regions (R) located at the 5′ and 3′ ends of the genomes (Fig. 1). Sequences of MPXVs and related OPXVs were obtained from Genbank (GB: DQ011157, DQ011154, NC001611, NC006998 and AY603355) and analyzed using bioinformatic tools. Genomic regions were selected based on mutation rates and presence of large-scale evolutionary events such as genomic rearrangement, inversion, truncation, insertion, and deletion. Additionally, each genomic region was selected by its degree of divergence between related viruses and its density of known virulence genes (Fig. 1 and Table 1). Through this analysis, two genomic regions were selected for in-depth analysis (Fig. 1). Three recombinant viruses (MPXV-ΔR1, MPXV-ΔR2, and MPXV-ΔR1/R2) containing deletions of individual or combined genomic regions were constructed (Fig. 2). Recombinant viruses were plaque purified, titered and assayed by cell culture and *in vivo* imaging.

Deletion of genomic regions in MPXV affected the replication kinetics and plaque size in cell culture

One-step growth curves and plaque size measurements were used to evaluate whether the deletion of genomic regions in MPXV affected *in vitro* growth and other phenotypic characteristics of gene-deleted viruses. Deletion of target genomic regions in MPXV reduced the *in vitro* growth characteristics of two of the recombinant viruses. MPXV-ΔR1 and MPXV-ΔR1/R2 viruses showed significant reduction in viral replication and total yield, as well as cell-to-cell spread. At 24, 48, and 72 h post-infection (pi), MPXV-ΔR1 and MPXV-ΔR1/R2 replicated to significantly lower peak titers ($p < 0.001$) and formed significantly smaller mean plaque sizes ($p < 0.01$) as compared to parental MPXV-Congo/Luc+ (Fig. 3A and B respectively). Interestingly, for MPXV-ΔR2 virus, the growth kinetics in cell culture appeared normal and comparable to parental MPXV-Congo/Luc+. The lag and rise periods of exponential growth curves were of similar duration along with peak titers (Fig. 3A). In addition, MPXV-ΔR2 virus did not differ in plaque size when compared to the parental MPXV-Congo/Luc+ (Fig. 3B). One-step growth curves in A549 cells showed similar results to Vero cells; however no differences in plaque phenotype were observed between parental and gene-deleted MPXVs (data not shown).

In vivo imaging demonstrated MPXV attenuation by deletion of genomic regions

Biophotonic *in vivo* imaging of CAST/EiJ mice was used to determine the pathogenicity of MPXV-ΔR1, MPXV-ΔR2, and MPXV-ΔR1/R2. At day 4 pi, viral spread and increased viral replication was seen in MPXV-Congo/Luc+ infected mice as compared to all of the gene-deleted viruses (Figs. 4 and 5A). Viruses containing deletions did not show signals of viral spread at day 4 pi. Between day 6 and 8 pi, morbidity, high viral replication, and generalized viral dissemination were observed in the control MPXV-Congo/Luc+ group (Figs. 4 and 5). All MPXV-Congo/Luc+ infected mice died or were euthanized by 8 days pi (Fig. 4). Only animals infected with parental MPXV-Congo/Luc+ exhibited significant weight loss ($p < 0.01$) (Fig. 5B). Weight change was not significantly different between groups of mice infected with MPXV

Table 1
Genes contained in the two MPXV genomic regions and their reported functions.

Deletion	[a]Location (ORF)	[b]MPXV/ VACV	Function
Region R1	17	D9L/C9L	Ankyrin-like
	18	D10L/C7L	Inhibits type I – IFN signaling (Meng et al., 2009, 2012)
	19	D11L/C6L	Unknown
	20	D12L/C5L	BTB domain of VACV C2L gene associated with adhesion and inflammation (Pires de Miranda et al., 2003)
	21	D13L/C4L	Unknown
	22	D14L/C3L	Regulates complement activation (Hudson et al., 2012; McKenzie et al., 1992)
	23–25	D18L/C2L	Kelch-like protein: absent or truncated in West African MPXV (Pires de Miranda et al., 2003)
	26	D19L/C1L	Unknown
	27	P1L/N1L	Inhibits apoptosis and NF-κB activation (Maluquer de Motes et al., 2011)
	28	P2L/N2L	α-amanitin-resistant and temperature-sensitive phenotypes (Tamin et al., 1991)
	29	O1L/M1L	Ankyrin-like
	30	O2L/M2L	Inhibits NF-κB activation *via* ERK2 signaling (Gedey et al., 2006)
	31	C1L/K1L	Inhibits NF-κB activation preventing IκBα degradation (Shisler and Jin, 2004)
Region R2	181	B7R/B6R	Ankyrin-like
	182	B8R/B7R	Modulator of virulence (Price et al., 2000)
	183	B9R/B8R	Soluble INF-gamma receptor-like protein (Verardi et al., 2001)
	184	B10R/B9R	Host defense modulator (Price et al., 2002)
	185	–/B11R	Unknown
	186	B11R/B12R	Ser/thr protein kinase-like similar to VACV B1R gene an apoptosis inhibitor (Banham and Smith, 1993; Santos et al., 2006)
	187	B12R/B13R	Apoptosis inhibidor: SPI-2/crmA, IL-1 convertase (Kettle et al., 1997)
	188	B13R/B15R	Unknown
	189	B14R/B15R	Host defense modulator : IL-1beta inhibitor (Alcami and Smith, 1992)
	190	B15R/B17L	Unknown: absent in West African MPXV
	191	–/B17L	Unknown: absent in West African MPXV
	192	B16R/B19R	IFN-alpha/beta-receptor-like secreted glycoprotein (Fernandez de Marco Mdel et al., 2010; Gomez et al., 2012)

[a] Open Reading Frames: GeneBank, DQ011154 (MPXV strain RCG/2003-358).
[b] Nomenclature from GeneBank sequences DQ011154 and NC006998 (VACV strain Western Reserve).

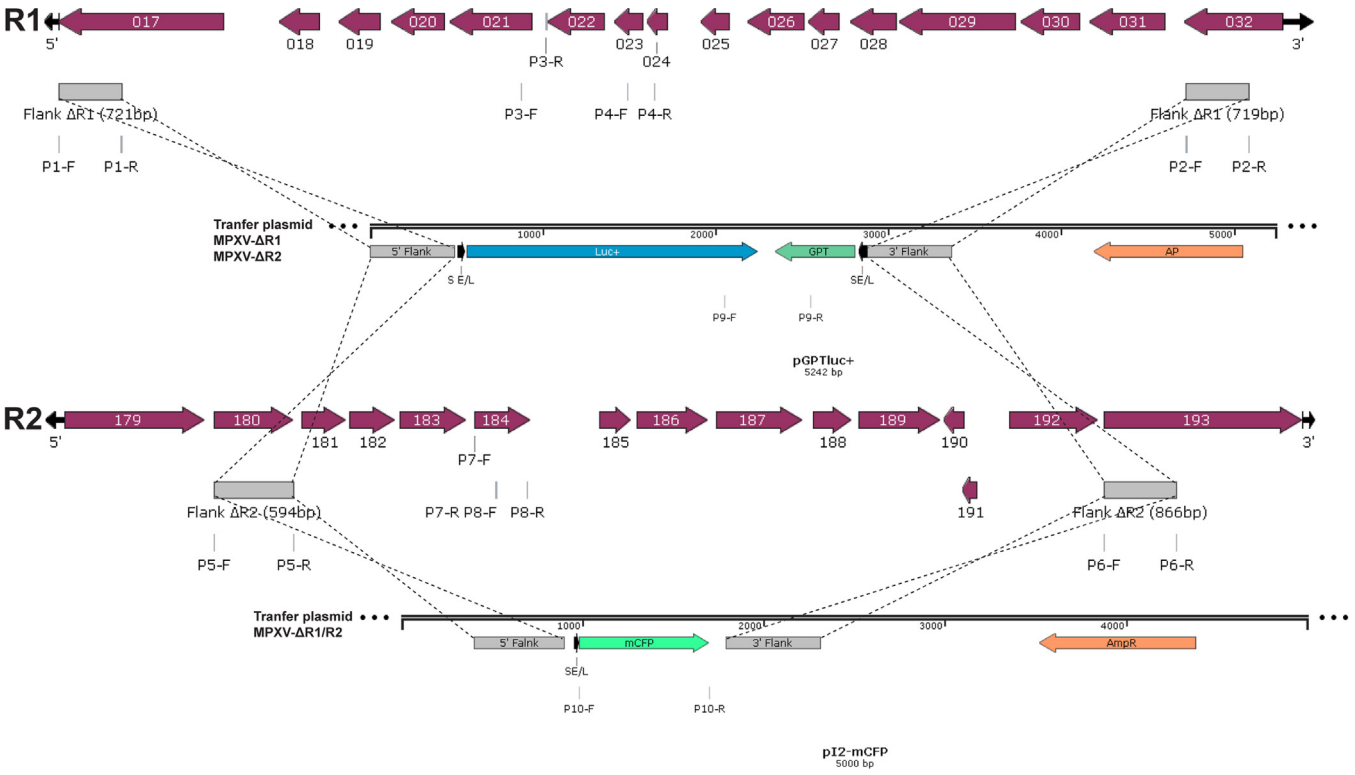

Fig. 2. Overview of recombination approach used to delete genomic regions in MPXV. The orientation of genes in the MPXV genome and luciferase and selection markers (GPT and CFP) in the transfer plasmids are noted by arrows. Flanking sequences of genomic regions are represented by rectangular bars. Dashed lines indicate the location of recombination within the MPXV genome and transfer plasmid in each genomic region. GenBank MPXV genomic sequences were utilized to clone the flank regions (DQ011154). Numbers indicate the corresponding open reading frames (ORFs) in the reference sequence. Locations of the primers used are represented by primer number (P). SnapGene® software (from GSL Biotech; available at snapgene.com) was used to generate the maps of the genomic deletions.

with deletions (Fig. 5B). Significant differences ($p < 0.01$) in luminescence were detected between gene-deleted viruses at days 6, 8, and 10 pi (Figs. 4 and 5A). Luminescent signal peaked on day 6 pi in mice infected with MPXV-ΔR1 or MPXV-ΔR2 (Figs. 4 and 5A). Animals infected with the MPXV-ΔR1/R2 showed a significant reduction ($p < 0.001$) at days 6 and 8 pi in viral replication and

spread as compared with MPXV-ΔR1 and MPXV-ΔR2, indicating an additive effect of deletion of genes in both genomic regions (Figs. 4 and 5A). All the mice infected with gene-deleted viruses survived infection; after 20 days pi none of the mice had detectable levels of luminescence and were therefore euthanized. Real-time PCR and tissue culture of lung and spleen confirmed the absence of viral DNA and lack of tissue persistence (data not shown). No differences in end point antibody titers between MPXV-ΔR1, MPXV-ΔR2, and MPXV-ΔR1/R2 were observed (Fig. 6A). However, serum of mice infected with MPXV-ΔR1/R2 had lower neutralizing antibody titers when compared with serum of mice from MPXV-ΔR1 and MPXV-ΔR2 infection (Fig. 6B).

Histopathology and viral titrations

Tissues were collected at the time of death or euthanasia: 7–8 days pi for the MPXV-Congo/Luc+ and at the completion of the study (20 days pi) for mice infected with gene-deleted viruses. Histological examination of spleens from mice infected with MPXV-Congo/Luc+ showed moderate to severe multifocal to coalescing lymphoid necrosis (Fig. 7A). Viral inclusions were occasionally found in active, enlarged macrophages. Virus titers in spleens of mice infected with MPXV-Congo/Luc+ ranged from 1.68×10^3 to 2.18×10^7 PFU/ml (data not shown). In contrast, spleens from MPXV-ΔR1 infected mice showed no loss of lymphoid cells. Lymphoid hyperplasia was present in spleens from MPXV-ΔR2 and MPXV-ΔR1/R2 infected mice (Figs. 7C and 7E). Lungs from MPXV-Congo/Luc+ infected mice showed severe multifocal lymphoplasmacytic pneumonia (Fig. 7B) with virus titers that ranged from 4.35×10^6 to 2.57×10^7 PFU/ml (data not shown). More severely affected animals showed severe necrosis in a peri-bronchiolar pattern, with fibrin filling some bronchioles and many alveoli. Lung tissue sections from mice infected with the MPXV containing region deletions had very mild lymphoplasmacytic infiltrates in all three groups (Fig. 7D). MPXV was not detected by either real-time PCR or tissue culture isolation from lung and spleen homogenates of animals infected with gene-deleted MPXVs (data not shown).

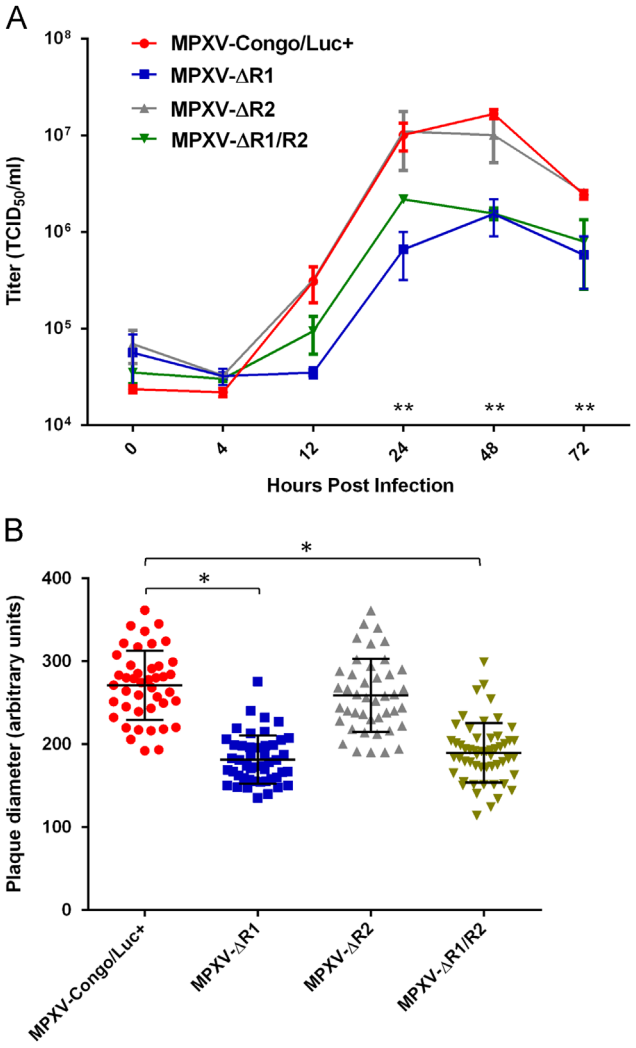

Fig. 3. Deletions of genomic regions in MPXV reduce replication and spread in cell culture. A) One step growth curves for parental virus (MPXV-Congo/Luc+) and viruses with single deletions (MPXV-ΔR1 and MPXV-ΔR2) and simultaneous deletion of both regions (MPXV-ΔR1/R2). Vero cells in 12-well plates were infected in duplicate with the recombinant viruses at MOI of 5 PFU/cell. Cells from each well were harvested at 0, 4, 12, 24, 48, and 72 h post-infection (pi). All samples including pellet and supernatants were titered by 50% tissue culture infective dose ($TCID_{50}$). Mean titers are shown at different times. Error bars represent the standard deviations (SD) of the replicates. B) Plaque size comparisons between control MPXV-Congo/Luc+ and gene-deleted viruses. Vero cells in 6-well plates were infected with the indicated viruses, and at 72 h pi cells were fixed and stained. The diameters of 40 plaques were measured for each virus. Data are expressed as the mean and SD of plaque diameter. Stars in the figures represent significant differences ($^*p < 0.01$ and $^{**}p < 0.001$) compared to control MPXV-Congo/Luc+ results.

Discussion

Experimental deletion of individual and multiple genes in OPXV genomes has been used to study virulence factors as well as to improve the immunogenicity and safety of vaccine vectors (Dimier et al., 2011; Johnston and McFadden, 2004; Kochneva et al., 2005). These studies have shown that deletion of individual genes can either reduce (Johnston and McFadden, 2004; Senkevich et al., 1994) or enhance (Estep et al., 2011; Ng et al., 2001) replication and virulence. Previous studies that investigated differences in virulence of MPXV strains have predominantly focused on the function and characterization of individual genes, for example, the inhibitor of complement-binding protein (MOPICE), an important anti-inflammatory factor of OPXV (Estep et al., 2011; Hudson et al., 2012). The gene that codes for these enzymes (D14R) is absent in the less virulent West African MPXV strains and has been considered a major virulence factor in Central African MPXV clade infection (Chen et al., 2005). Results showed that deletion of D14R in Central African MPXV clade enhanced viral replication in rhesus macaques (Estep et al., 2011). Another report showed that deletion of D14R in Central African MPXV clade subtly reduced morbidity and mortality in prairie dogs, and D14R insertion in West African MPXV clade only affected minor disease manifestations (Hudson et al., 2012). Similar to these previous reports, we have observed that the single deletion of MOPICE gene and B14R gene, an inhibitor of IL-1β-binding protein, in MPXV/Congo increased viral replication and spread after intranasal inoculation of CAST/EiJ and severe combined immunodeficiency (SCID) mice, respectively (Lopera et al., unpublished data). These studies suggested that D14R or B14R are not the sole virulence factors responsible for major differences in MPX pathogenesis (Estep et al., 2011; Hudson et al., 2012).

Here, we used a larger genomic approach to generate MPXV with deletion of multiple virulence genes in order to evaluate their roles in viral replication and pathogenicity. We found that single and double deletion of two specific genomic regions in a MPXV strain from Central Africa affected the cell culture phenotype (MPXV-ΔR1 and MPXV-ΔR1/R2) and reduced morbidity and mortality in mice (MPXV-ΔR1, MPXV-ΔR2 and MPXV-ΔR1/R2).

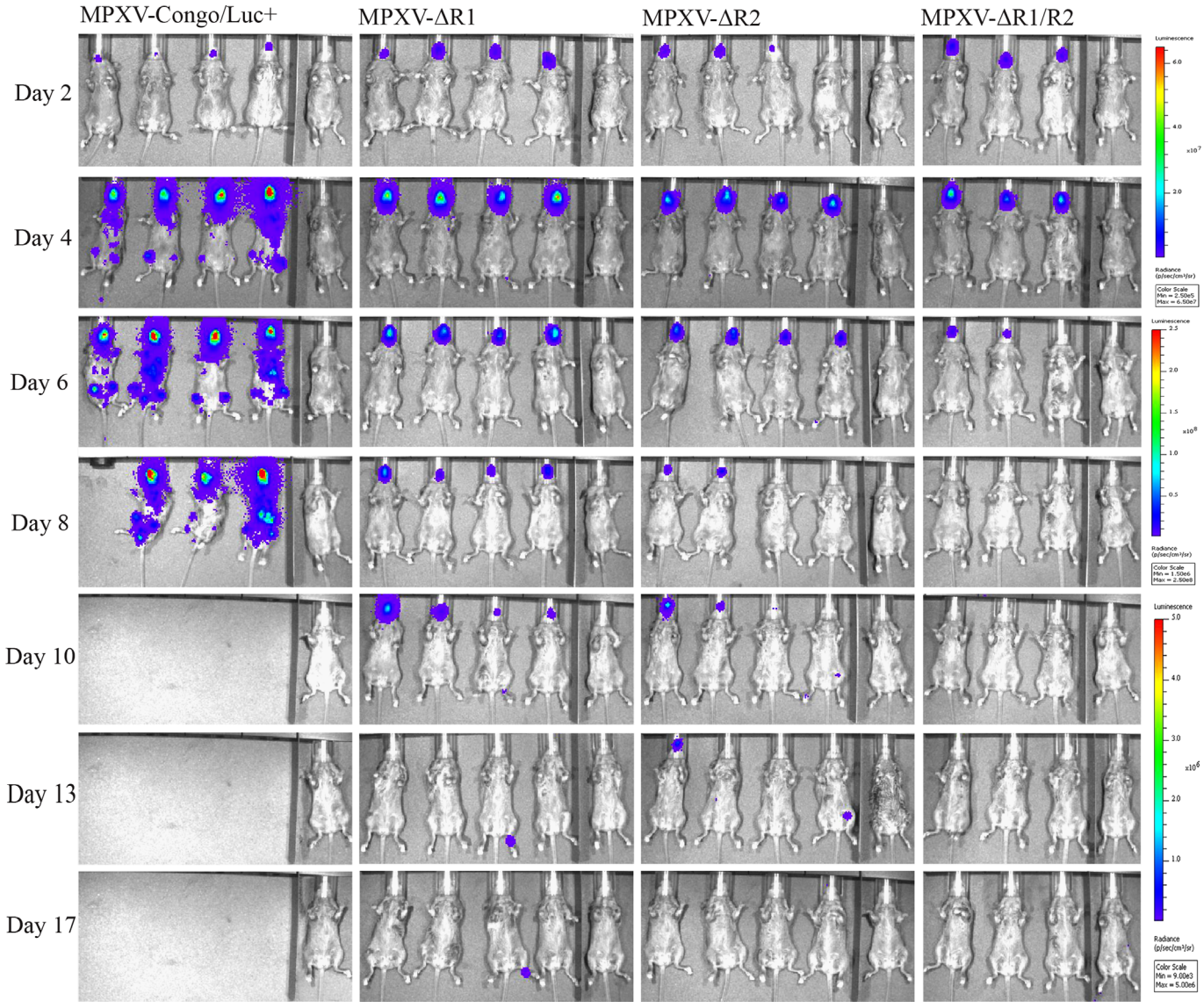

Fig. 4. *In vivo* imaging of luminescent gene-deleted viruses shows attenuation in CAST/EiJ mice. Ventral views of mice (CAST/EiJ) infected intranasally with 10^6 PFU of parental (MPXV-Congo/Luc+) or gene-deleted MPXVs (MPXV-ΔR1, MPXV-ΔR2, and MPXV-ΔR1/R2) that express firefly luciferase gene marker. Viral replication, course of infection (*in vivo* imaging), weight loss, and deaths were recorded in infected animals for 20 days.

All the gene-deleted viruses characterized in this study were strongly attenuated *in vivo*, and further *in vivo* imaging and histological analysis confirmed the reduction in pathogenesis. It is possible that the observed attenuation of MPXV-ΔR1 virus could be explained, in part, by the reduced capacity of this virus to grow and spread in cell culture, indicating that genes in ΔR1 have important roles in MPXV replication. On the other hand, the observed *in vivo* attenuation of deletion from ΔR2 suggests that this specific genomic region contains important genes that affect MPXV pathogenicity. This result is supported by the observation that growth of MPXV-ΔR2 appeared normal in cell culture but was strongly attenuated *in vivo*. Evaluation of the reported function of genes deleted in ΔR2 showed that they encode for important immunomodulatory proteins, including secreted inhibitors of type I and type II interferons, an inhibitor of IL-1β, and two apoptosis modulators (Gomez et al., 2012; Jackson et al., 2005; Verardi et al., 2001). Finally, the robust attenuation caused by the deletion of ΔR1/R2, could be explained by both a reduction of the capacity of the virus to replicate and the ability to evade the early host immune responses. Thus, mice infected with MPXV-ΔR1/R2 showed reduction in viral replication and by day 8 pi the luciferase expression was absent, suggesting early viral detection and clearance by the host immune system. This finding was further supported by low levels of neutralizing antibodies induced by the MPXV-ΔR1/R2. Other studies that evaluated large scale deletions of OPXV genomic regions have shown that the deletion of six genomic regions in vaccinia virus (VACV) (31 open reading frames) was not sufficient to reduce cell culture replication and mice virulence of a parental strain (Meisinger-Henschel et al., 2010). It is surprising that deletion of these large numbers of genes in VACV, including some known OPXV virulence factors, has only moderate effects on the viral pathogenicity. Additionally, the deletion of two to four genomic regions enhanced the virulence in mice compared to the parental VACV (Meisinger-Henschel et al., 2010).

The evaluation of MPX disease progression by molecular imaging is an effective approach for the characterization of MPXV and other OPXV pathogenesis in mice and wild rodents (Americo et al., 2014; Falendysz et al., 2014; Osorio et al., 2009). Taking

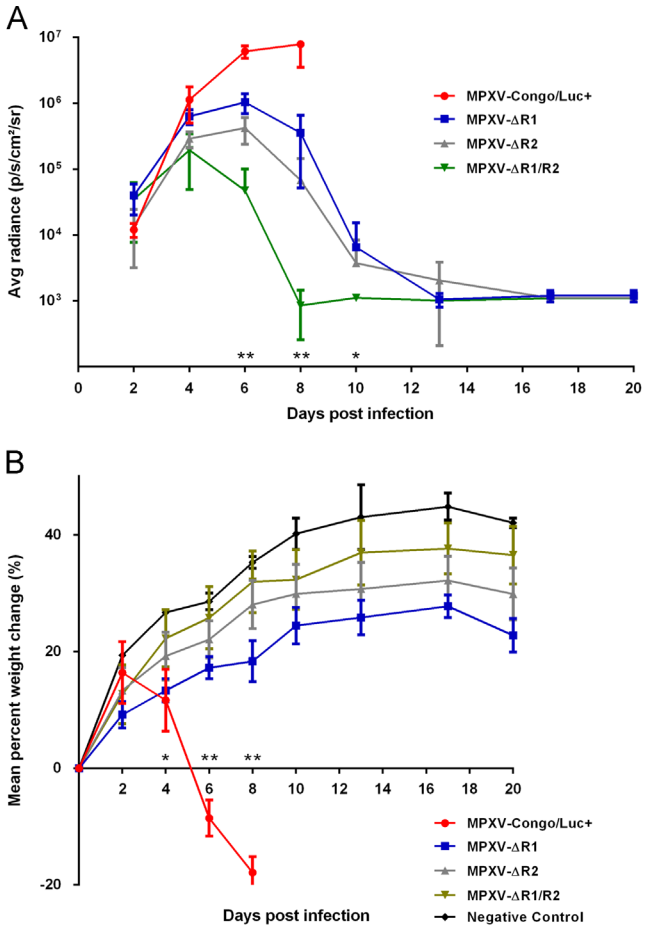

Fig. 5. Deletions of genomic regions in MPXV reduce morbidity and viral replication in CAST/EiJ mice. A) Mean and SD of luminescence measurements by time after infection. B) Mean and SD of weight change of mice in each experimental group collected at different times after the infection. Stars in the figures represent significant differences ($^{*}p < 0.01$ and $^{**}p < 0.001$) compared to control MPXV-Congo/Luc+ results.

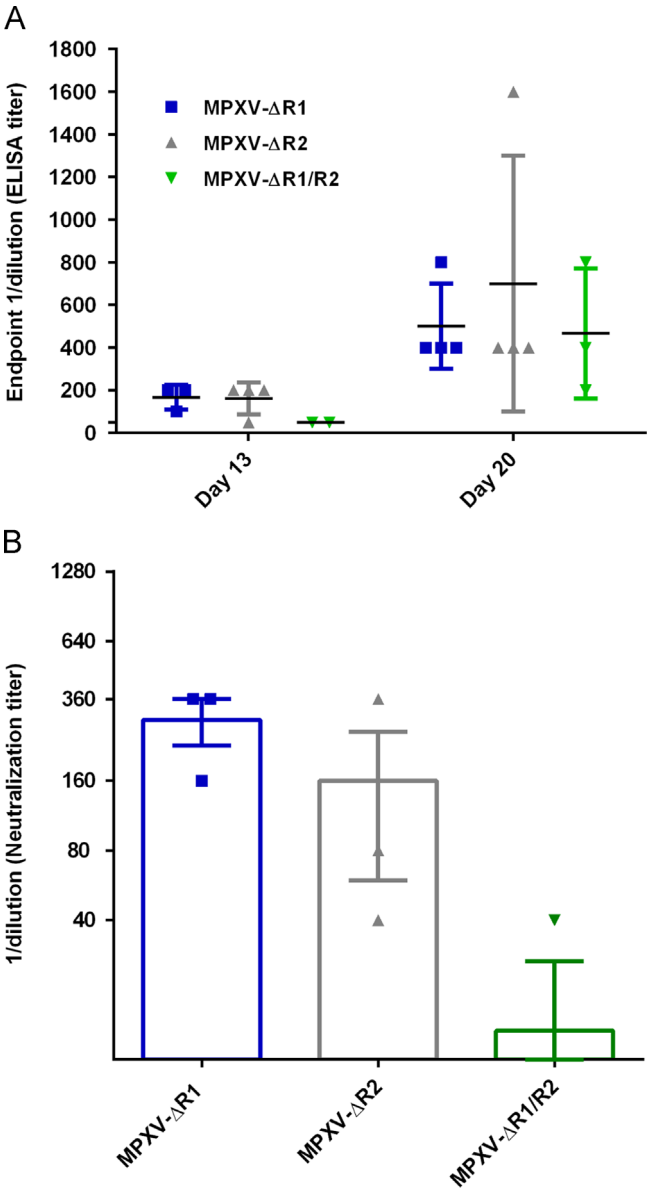

Fig. 6. Comparison of humoral responses. A) Serological analysis of CAST/EiJ mice infected with gene-deleted viruses shows similar antibody titers. Titers of binding antibodies against MPXV were determined by ELISAs using anti-OPXV immunoglobulin types A and G. B) Percent of neutralizing activity of serum of mice infected with gene-deleted viruses display differences in neutralization activity. Bars represent the mean and SD of endpoint titer and percent of neutralization for individual animals in each experimental group.

advantage of the incorporation of the luciferase gene reporter system, we used *in vivo* biophotonic imaging to characterize and compare MPX disease progression and viral replication in a susceptible CAST/EiJ mouse model. Previous mouse models such as SCID, Balb/c, A129 and AG129 mice were not useful for the characterization of MPXV virulence factors (Hutson et al., 2010; Hutson and Damon, 2010), because these animals do not succumb to MPXV infection, and differences in mortality and morbidity are difficult to observe. Our data showed that the CAST/EiJ animal model is useful for studying MPXV virulence factors, as well as the host immune response. However, other animal models, such as prairie dogs, could display clinical signs that more closely representing MPX disease in humans (Falendysz et al., 2014). Future studies will use the prairie dog model to study the effects of deletions on clinical signs and progression of MPX disease in a more relevant outbred model. Bioinformatic analysis revealed the presence of other divergent genomic regions and to understand the relative contribution of multiple genes on MPXV replication and pathogenicity, additional studies are needed.

Conclusion

In this study we described the construction and characterization of large scale deletions of genes in MPXV and evaluated their effect on disease pathogenesis in mice. We conclude that deletion of individual (ΔR1 and ΔR2) and dual (ΔR1/R2) target genomic regions in MPXV-Congo affect viral replication and/or pathogenicity. Deletion of R1 affected viral replication, whereas deletion of R2 had a more marked effect on disease pathogenesis. The marked attenuation of viruses with simultaneous deletion of two regions (MPXV-ΔR1/R2) illustrates the additive effect of deletion of genomic regions in viral replication and pathogenicity. The mechanisms by which multiple genes modulate host pathogenesis and immune response have not been evaluated, and we will further characterize the additive function of these genes in MPXV infection. Collectively, our results strongly suggest that the use of parental and mutant deleted MPXV/Luc+ can be a safe and useful tool with several potential advantages for the study of MPX pathogenesis.

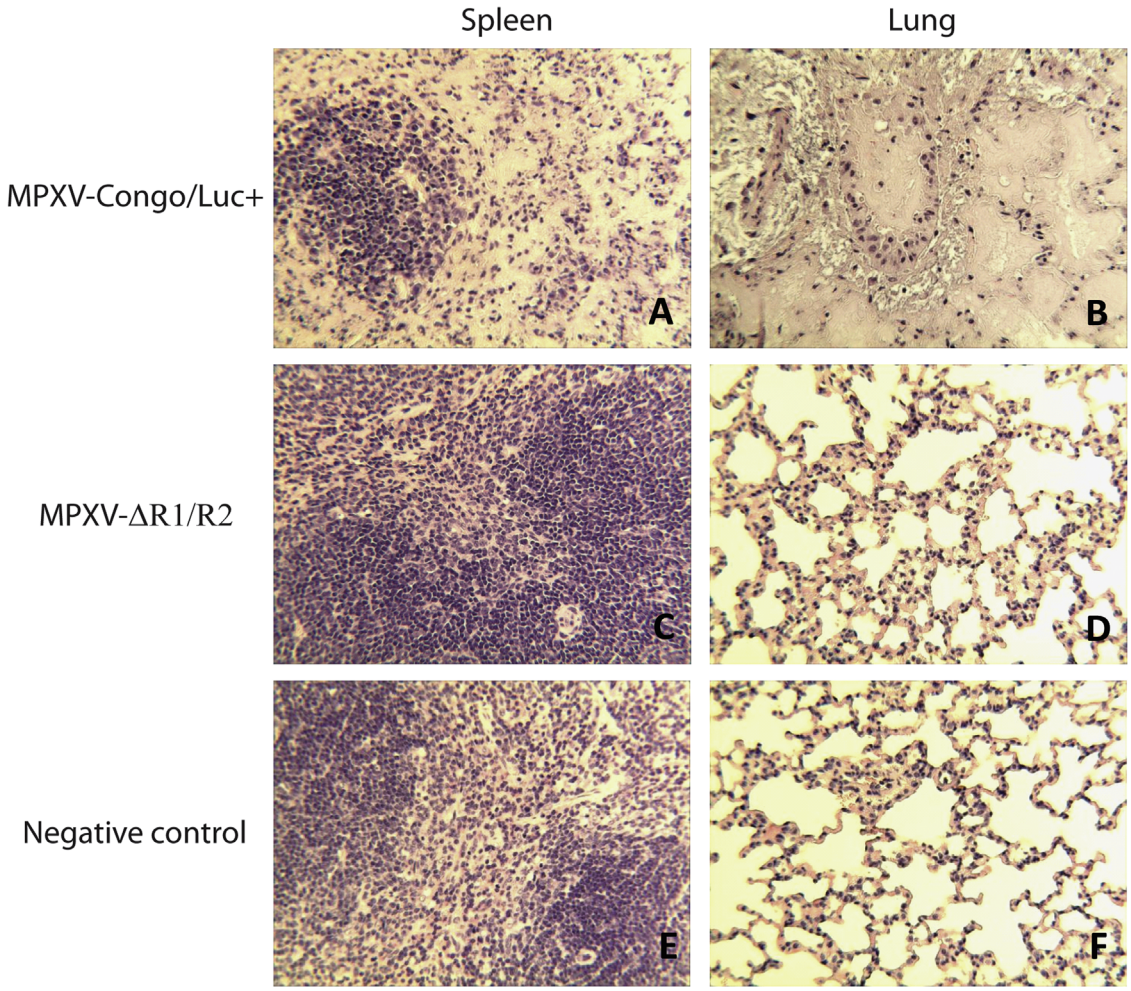

Fig. 7. Hematoxylin and eosin stained spleens and lungs of infected and control CAST/EiJ mice (25 ×). Spleens of animals infected with parental MPXV-Congo/Luc+ (A) displayed severe lymphoid necrosis with loss of much of the germinal centers and replacement with adipose tissue. Spleens of animals infected with the double deletion, MPXV-ΔR1/R2 (C), have widened germinal centers, indicative of lymphoid hyperplasia. Spleens of uninfected mice display smaller germinal centers with discrete separation of white pulp and red pulp (E). Lungs of mice infected with MPX-Congo/Luc+ (B) had severe multifocal lymphocytic pneumonia with necrosis and copious fibrin present in the bronchioles and alveoli. Lungs of MPXV-ΔRl/R2, had sparse lymphocytic infiltrates (D). Lung of an uninfected control mouse (F).

Materials and methods

Viruses, cells and animals

The parental MPXV strain Congo-2003-358 (MPXV/Congo) was provided by Dr. Inger K. Damon (Centers for Disease Control, Atlanta, GA, USA). All studies were conducted under BSL-3 conditions at the USGS, National Wildlife Health Center – Madison (NWHC, Madison, WI, USA). Experimental protocols were approved by the NWHC biosafety committee. Virus titration and propagation were conducted in African green monkey kidney epithelial cells (Vero and BS-C-1) and human alveolar epithelial cells (A549) obtained from American Type Culture Collection (ATCC: CCL81, CCL-26 and CCL-185). Virus titers were calculated by plaque assays and were performed using 12-well plates of Vero cells incubated under semisolid overlay (cell culture medium containing 2% FBS and 1.5% carboxymethylcellulose) for 72 h. All cells were maintained with the ATCC recommended culture media at 37 °C and 5% CO_2. Plates were fixed and plaques were visualized by staining with 0.1% crystal violet in 10% neutral buffered formalin. Mouse studies were conducted using 4 week-old female CAST/EiJ mice purchased from the Jackson Laboratories (Bar Harbor, ME). Animals were housed in cages with an aerosol filter and standard husbandry practices were performed in accordance with NWHC animal care and IACUC guidelines (Protocol # EP090616A). Virus titers were verified before and after the experiments to ensure the accuracy of the doses administered.

Bioinformatics analysis and generation of recombinant MPXVs

Genomic regions (R) in MPXV were identified by multiple genome alignments and sequence analysis using MAUVE and DAMBE software packages (Fig. 1) (Darling et al., 2010; Xia, 2013). MAUVE produces genomic alignments from which orthologous and divergent regions can be identified. These regions are then automatically categorized based on the degree of change, and fine-scale analyses of nucleotide and amino acid changes of individual genes were performed with DAMBE.

To generate mutant deleted viruses, transfer plasmids containing the luciferase gene marker (Luc+), the guanosine phosphoribosyl transferase (GPT) selection gene under the control of the synthetic early late promoter (SE/L), and the flanking sequences of target genomic regions were constructed using methods previously described (Osorio et al., 2009) (Fig. 2). Briefly, for MPXV with R1 deleted (MPXV-ΔR1), sequences for the left (721 bp) and right (719 bp) flanks were PCR amplified and cloned into transfer plasmids. For MPXV with R2 deleted (MPXV-ΔR2), sequences for the left (954 bp) and right (866 bp) flanks were PCR amplified and

Table 2
List of primer sequences used in construction, selection and purification of gene-deleted MPXV viruses.

Regions and Plasmids	Primers	Sequence 5′-3′	PCR product (bp)	Description
Region R1	P1-F	ttataggaacgcgtacgagaa	721	Left flank ΔR1
	P1-R	actaaaaatttgtaagccgtatat		
	P2-F	tacccataaacaatataaatccag	719	Right flank ΔR1
	P2-R	attaaactttagacgagatgcg		
	P3-F	tgtgtcggtagacgataccg	290	ΔR1 confirmation
	P3-R	caactacaatgtagactttaagtgc		
	P4-F	caccacaagaacacacgaacg	310	ΔR1 confirmation
	P4-R	ttcaggcgcatcagtattcg		
Region R2	P5-F	atgaaaacgatttccgttgttac	594	Left flank ΔR2
	P5-R	tcacggtagcaatttatggaact		
	P6-F	atggatgaagatacgcgactatc	866	Right flank ΔR2
	P6-R	attggatccttattactgctatcc		
	P7-F	agatgaggtccctgattatagtcc	259	ΔR2 confirmation
	P7-R	tcggtgataataaagtcatgtgg		
	P8-F	ccacatgactttattatcaccga	366	ΔR2 confirmation
	P8-R	acctttgtagacattacggtcg		
pGPTluc+	P9-F	gagcacggaaagacgatgac	500	Confirmation of luciferase gene insertion
	P9-R	tcgttattgatgacctggtgg		
pI2-mCFP	P10-F	atggtgagcaagggcgaggagc	720	Confirmation of fluorescence gene insertion
	P10-R	ttacttgtacagctcgtgcatgc		

cloned. For the construction and selection of MPXV with simultaneous deletion of both genomic regions (MPXV-ΔR1/R2), we used MPXV-ΔR1 as the parental virus and deleted R2 using a transfer plasmid containing cerulean fluorescent protein gene (CFP) as a selection marker with the same flanking sequences of the individual R2 deletion. Table 1 shows the composition, genomic location, and reported function of deleted genes in each genomic region. Sequencing, PCR, and luciferase assays showed that the gene-deleted viruses contained the intended deletions and the luciferase gene marker (data not shown). Sequences and binding sites of primers used in this study are listed in Table 2.

Kinetics of replication and plaque size phenotype

Twelve-well plates containing semi-confluent Vero and A549 cells were infected with each virus in duplicate, with a multiplicity of infection (MOI) of 5 plaque forming units (PFU) per cell. Cells were incubated for 45 min for virus adsorption, infection media was removed, and cells were washed twice with 1 × phosphate buffered saline (PBS). Fresh media was added and virus was harvested at 0, 4, 8, 12, 24, 48, and 72 h post-infection (pi) and stored at −80 °C. After three cycles of freezing and thawing, samples were sonicated and virus titers were determined by 50% tissue culture infective dose ($TCID_{50}$/ml) as described elsewhere (Falendysz et al., 2014). Plaque morphology was analyzed by performing plaque assays as described in the previous section. Plaque sizes ($n > 40$) were measured using ImagePro Plus 3.1 software (Media Cybernetics, USA) and an ImmunoSpot microscope (Cellular Technology Ltd, USA). Differences in virus titers and plaque diameters were plotted using GraphPad Prism software (La Jolla, CA). Student's *t*-test method was used to determine statistical significance, with alpha = 1%.

Inoculation of animals and sample collection

CAST/EiJ mice, which have been shown to be highly susceptible to MPXV infection (Americo et al., 2010; Earl et al., 2012), were used to characterize the effect of deletion of target genomic regions on MPXV pathogenicity. Groups ($n = 3$–4) of 4-week-old CAST/EiJ mice were inoculated intranasally (IN) with 10^6 PFU/0.01 ml of either MPXV-ΔR1, MPXV-ΔR2, or MPXV-ΔR1/R2. MPXV-Congo/Luc+ (same dose and route) served as a positive control. A group of two additional animals were inoculated with PBS as a negative control. We previously demonstrated that the insertion of the luciferase gene (Luc+) does not affect viral replication when compared to wild type MPXV-Congo (Osorio et al., 2009). Daily observation of food consumption, activity level, and general appearance was recorded. Viral replication, tissue tropism, and persistence were monitored by *in vivo* imaging. Bioluminescent imaging and weighing were performed on days 2, 4, 6, 8, 10, 13, 17, and 20 pi. Images were acquired with an IVIS 200 series *in vivo* imager (Perkin-Elmer, Waltham, MA). Additionally, serum samples were collected prior to infection and at days 13 and 20 pi to test for antibodies. Animals that lost 20% of their starting weight were euthanized in accordance with institutional animal care and use protocols. After death, lungs and spleen were removed; a portion of each organ was fixed in 10% neutral buffered formalin and remaining tissue was frozen at −80 °C for later PCR and viral titration.

Region of interest (ROI) analysis was performed using Living Image 4.2 (Perkin-Elmer, Waltham, MA) of rectangular ROIs that enclosed ventral views of individual animals. Total luminescence was estimated as mean average radiance [p/s/cm²/sr] of ventral views of individual mice and plotted with the time of infection. Mean percent of weight change for each experimental group was calculated and plotted over time. Differences in luminescence and weight change were compiled in Microsoft Excel files and analyzed using GraphPad Prism software. Student's *t*-test corrected for multiple comparisons with the Sidak–Bonferroni method was used to determine statistical significance, with alpha = 1%.

Real-time PCR and viral titration

To verify presence or absence of virus and quantify tissue titers in infected mice, tissues collected at the time of death or euthanasia were evaluated by real-time PCR and cell culture isolation assays. Tissue samples were homogenized using a Bullet Blender Storm bead homogenizer (Next Advance, Averill Park, NY) according to tissue-specific protocols (Next Advance, 2012). Total DNA was extracted from aliquots of 100 µl of tissue slurry using Quick-gDNA™ kit (ZYMO RESEARCH, Irvine, CA). Homogenized tissues were tested for the presence of viral DNA using real-time PCR to amplify the E9L gene of orthopoxviruses as described elsewhere (Li et al., 2010) with minor modifications. The remaining aliquots (100 µl) of the tissue slurry were evaluated for virus isolation and titration as described above.

Measure of antibody responses

Enzyme-linked immunosorbent assay (ELISA) and neutralizing activity assays were used to evaluate serum of mice infected with recombinant MPXVs. For measuring total IgG titers, individual serum samples collected at days 13 and 20 pi were tested as described elsewhere (Hutson et al., 2007). Briefly, 96-well microtiter plates were coated with crude viral antigen (lysate of Vero cells infected with VACV) and uninfected Vero cell lysate. Plates were blocked (PBS, 0.05% Tween-20, 5% dried skim milk, 2% normal goat serum, and 2% bovine serum albumin) for 1 h. Six serial 2-fold dilutions (1:50, 1:100, 1:200, 1:400, 1:800 and 1:1600) of serum were incubated in duplicate for 1 h at 37 °C. Plates were washed four times (PBS plus 0.05% Tween-20), and conjugated secondary antibody (Pierce ImmunoPure© Protein A/G Peroxidase conjugated) was added and incubated for 1 h at 37 °C. Peroxidase substrate was added and incubated for 15 min, at which point stop solution was added to cease the reaction before quantification. Absorbance was read on an ELISA reader at 450 nm. Samples were considered positive if the test absorbance was above the estimated cut-off value (COV), which was defined as three standard deviations above the mean of the negative controls. A luciferase based MPXV serum neutralization assay was used to test neutralizing antibody activity as described elsewhere (Liu et al., 2012). Briefly, samples were incubated in duplicate on 96-well plates for 1 h at 37 °C with 100 PFU/well of MPXV-Congo/Luc+ and six serial 2-fold dilutions (1:40, 1:80, 1:160, 1:340, 1:680 and 1:1280) of serum. Then, cells were incubated (virus and serum dilutions) for 24 h, lysed, and reduction in luminescence was measured using a plate luminometer (VICTOR® Light 1420 luminescence counter, Perkin-Elmer, Waltham, MA, USA). To ensure the specificity of the assay conditions, positive and negative sera were used to normalize the ELISA titers and luminescence readings. All reported values represent the average of duplicate samples. Serum samples of CAST/EiJ mice infected with a sublethal dose (10^2 PFU) of parental MPXV-Congo/Luc+ from previous studies were used as positive controls, and serum from an uninfected mouse was utilized as a negative control.

Histopathology

After death or euthanasia, necropsy was performed on all groups to evaluate tissue pathology. Fixed tissue sections from the lung and spleen of control and infected animals were stained with hematoxylin and eosin (H&E) and histological changes were assessed.

Acknowledgments

We are grateful to Dr. Matthew Aliota, Dr. Rachel Abbott, James Weger-Lucarelli and Steve Scahill for excellent reviews of the manuscript. This work was sponsored by NIH, United States Grant 1-U54-AI-057153. Use of trade, product, or firm names does not imply endorsement by the U.S. Government.

References

Alcami, A., Smith, G.L., 1992. A soluble receptor for interleukin-1 beta encoded by vaccinia virus: a novel mechanism of virus modulation of the host response to infection. Cell 71, 153–167.

Americo, J.L., Moss, B., Earl, P.L., 2010. Identification of wild-derived inbred mouse strains highly susceptible to monkeypox virus infection for use as small animal models. J. Virol. 84, 8172–8180.

Americo, J.L., Sood, C.L., Cotter, C.A., Vogel, J.L., Kristie, T.M., Moss, B., Earl, P.L., 2014. Susceptibility of the wild-derived inbred CAST/Ei mouse to infection by orthopoxviruses analyzed by live bioluminescence imaging. Virology 449, 120–132.

Banham, A.H., Smith, G.L., 1993. Characterization of vaccinia virus gene B12R. J. Gen. Virol. 74 (Pt 12), 2807–2812.

Breman, J.G., Henderson, D.A., 1998. Poxvirus dilemmas–monkeypox, smallpox, and biologic terrorism. N. Engl. J. Med. 339, 556–559.

Cann, J.A., Jahrling, P.B., Hensley, L.E., Wahl-Jensen, V., 2013. Comparative pathology of smallpox and monkeypox in man and macaques. J. Comp. Pathol. 148, 6–21.

Chen, N., Li, G., Liszewski, M.K., Atkinson, J.P., Jahrling, P.B., Feng, Z., Schriewer, J., Buck, C., Wang, C., Lefkowitz, E.J., Esposito, J.J., Harms, T., Damon, I.K., Roper, R.L., Upton, C., Buller, R.M., 2005. Virulence differences between monkeypox virus isolates from West Africa and the Congo basin. Virology 340, 46–63.

Darling, A.E., Mau, B., Perna, N.T., 2010. progressiveMauve: multiple genome alignment with gene gain, loss and rearrangement. PloS One 5, e11147.

Dimier, J., Ferrier-Rembert, A., Pradeau-Aubreton, K., Hebben, M., Spehner, D., Favier, A.L., Gratier, D., Garin, D., Crance, J.M., Drillien, R., 2011. Deletion of major nonessential genomic regions in the vaccinia virus Lister strain enhances attenuation without altering vaccine efficacy in mice. J. Virol. 85, 5016–5026.

Earl, P.L., Americo, J.L., Moss, B., 2012. Lethal monkeypox virus infection of CAST/EiJ mice is associated with a deficient gamma interferon response. J. Virol. 86, 9105–9112.

Estep, R.D., Messaoudi, I., O'Connor, M.A., Li, H., Sprague, J., Barron, A., Engelmann, F., Yen, B., Powers, M.F., Jones, J.M., Robinson, B.A., Orzechowska, B.U., Manoharan, M., Legasse, A., Planer, S., Wilk, J., Axthelm, M.K., Wong, S.W., 2011. Deletion of the monkeypox virus inhibitor of complement enzymes locus impacts the adaptive immune response to monkeypox virus in a nonhuman primate model of infection. J. Virol. 85, 9527–9542.

Falendysz, E.A., Londono-Navas, A.M., Meteyer, C.U., Pussini, N., Lopera, J.G., Osorio, J.E., Rocke, T.E., 2014. Evaluation of monkeypox virus infection of black-tailed prairie dogs (Cynomys ludovicianus) using *in vivo* bioluminescent imaging. J. Wildl. Dis. 50, 524–536.

Fernandez de Marco Mdel, M., Alejo, A., Hudson, P., Damon, I.K., Alcami, A., 2010. The highly virulent variola and monkeypox viruses express secreted inhibitors of type I interferon. FASEB J.: Off. Publ. Fed. Am. Soc. Exp. Biol. 24, 1479–1488.

Gedey, R., Jin, X.L., Hinthong, O., Shisler, J.L., 2006. Poxviral regulation of the host NF-kappaB response: the vaccinia virus M2L protein inhibits induction of NF-kappaB activation via an ERK2 pathway in virus-infected human embryonic kidney cells. J. Virol. 80, 8676–8685.

Gomez, C.E., Perdiguero, B., Najera, J.L., Sorzano, C.O., Jimenez, V., Gonzalez-Sanz, R., Esteban, M., 2012. Removal of vaccinia virus genes that block interferon type I and II pathways improves adaptive and memory responses of the HIV/AIDS vaccine candidate NYVAC-C in mice. J. Virol. 86, 5026–5038.

Hammarlund, E., Dasgupta, A., Pinilla, C., Norori, P., Fruh, K., Slifka, M.K., 2008. Monkeypox virus evades antiviral CD4+ and CD8+ T cell responses by suppressing cognate T cell activation. Proc. Natl. Acad. Sci. USA 105, 14567–14572.

Hendrickson, R.C., Wang, C., Hatcher, E.L., Lefkowitz, E.J., 2010. Orthopoxvirus genome evolution: the role of gene loss. Viruses 2, 1933–1967.

Hudson, P.N., Self, J., Weiss, S., Braden, Z., Xiao, Y., Girgis, N.M., Emerson, G., Hughes, C., Sammons, S.A., Isaacs, S.N., Damon, I.K., Olson, V.A., 2012. Elucidating the role of the complement control protein in monkeypox pathogenicity. PloS One 7, e35086.

Huhn, G.D., Bauer, A.M., Yorita, K., Graham, M.B., Sejvar, J., Likos, A., Damon, I.K., Reynolds, M.G., Kuehnert, M.J., 2005. Clinical characteristics of human monkeypox, and risk factors for severe disease. Clin. Infect. Dis.: Off. Publ. Infect. Dis. Soc. Am. 41, 1742–1751.

Hutson, C.L., Abel, J.A., Carroll, D.S., Olson, V.A., Braden, Z.H., Hughes, C.M., Dillon, M., Hopkins, C., Karem, K.L., Damon, I.K., Osorio, J.E., 2010. Comparison of West African and Congo Basin monkeypox viruses in BALB/c and C57BL/6 mice. PloS One 5, e8912.

Hutson, C.L., Damon, I.K., 2010. Monkeypox virus infections in small animal models for evaluation of anti-poxvirus agents. Viruses 2, 2763–2776.

Hutson, C.L., Lee, K.N., Abel, J., Carroll, D.S., Montgomery, J.M., Olson, V.A., Li, Y., Davidson, W., Hughes, C., Dillon, M., Spurlock, P., Kazmierczak, J.J., Austin, C., Miser, L., Sorhage, F.E., Howell, J., Davis, J.P., Reynolds, M.G., Braden, Z., Karem, K.L., Damon, I.K., Regnery, R.L., 2007. Monkeypox zoonotic associations: insights from laboratory evaluation of animals associated with the multi-state US outbreak. Am. J. Trop. Med. Hyg. 76, 757–768.

Jackson, S.S., Ilyinskii, P., Philippon, V., Gritz, L., Yafal, A.G., Zinnack, K., Beaudry, K.R., Manson, K.H., Lifton, M.A., Kuroda, M.J., Letvin, N.L., Mazzara, G.P., Panicali, D.L., 2005. Role of genes that modulate host immune responses in the immunogenicity and pathogenicity of vaccinia virus. J. Virol. 79, 6554–6559.

Johnston, J.B., McFadden, G., 2004. Technical knockout: understanding poxvirus pathogenesis by selectively deleting viral immunomodulatory genes. Cell. Microbiol. 6, 695–705.

Kettle, S., Alcami, A., Khanna, A., Ehret, R., Jassoy, C., Smith, G.L., 1997. Vaccinia virus serpin B13R (SPI-2) inhibits interleukin-1beta-converting enzyme and protects virus-infected cells from TNF- and Fas-mediated apoptosis, but does not prevent IL-1beta-induced fever. J. Gen. Virol. 78 (Pt 3), 677–685.

Kindrachuk, J., Arsenault, R., Kusalik, A., Kindrachuk, K.N., Trost, B., Napper, S., Jahrling, P.B., Blaney, J.E., 2012. Systems kinomics demonstrates Congo Basin monkeypox virus infection selectively modulates host cell signaling responses as compared to West African monkeypox virus (M111 015701). Mol. Cell. Proteomics 11, M1105701.

Kochneva, G., Kolosova, I., Maksyutova, T., Ryabchikova, E., Shchelkunov, S., 2005. Effects of deletions of kelch-like genes on cowpox virus biological properties. Arch. Virol. 150, 1857–1870.

Li, Y., Zhao, H., Wilkins, K., Hughes, C., Damon, I.K., 2010. Real-time PCR assays for the specific detection of monkeypox virus West African and Congo Basin strain DNA. J. Virol. Methods 169, 223–227.
Likos, A.M., Sammons, S.A., Olson, V.A., Frace, A.M., Li, Y., Olsen-Rasmussen, M., Davidson, W., Galloway, R., Khristova, M.L., Reynolds, M.G., Zhao, H., Carroll, D. S., Curns, A., Formenty, P., Esposito, J.J., Regnery, R.L., Damon, I.K., 2005. A tale of two clades: monkeypox viruses. J. Gen. Virol. 86, 2661–2672.
Liu, Q., Huang, W., Nie, J., Zhu, R., Gao, D., Song, A., Meng, S., Xu, X., Wang, Y., 2012. A novel high-throughput vaccinia virus neutralization assay and preexisting immunity in populations from different geographic regions in China. PloS One 7, e33392.
Maluquer de Motes, C., Cooray, S., Ren, H., Almeida, G.M., McGourty, K., Bahar, M.W., Stuart, D.I., Grimes, J.M., Graham, S.C., Smith, G.L., 2011. Inhibition of apoptosis and NF-kappaB activation by vaccinia protein N1 occur via distinct binding surfaces and make different contributions to virulence. PLoS Pathog. 7, e1002430.
McKenzie, R., Kotwal, G.J., Moss, B., Hammer, C.H., Frank, M.M., 1992. Regulation of complement activity by vaccinia virus complement-control protein. J. Infect. Dis. 166, 1245–1250.
Meisinger-Henschel, C., Spath, M., Lukassen, S., Wolferstatter, M., Kachelriess, H., Baur, K., Dirmeier, U., Wagner, M., Chaplin, P., Suter, M., Hausmann, J., 2010. Introduction of the six major genomic deletions of modified vaccinia virus Ankara (MVA) into the parental vaccinia virus is not sufficient to reproduce an MVA-like phenotype in cell culture and in mice. J. Virol. 84, 9907–9919.
Meng, X., Jiang, C., Arsenio, J., Dick, K., Cao, J., Xiang, Y., 2009. Vaccinia virus K1L and C7L inhibit antiviral activities induced by type I interferons. J. Virol. 83, 10627–10636.
Meng, X., Schoggins, J., Rose, L., Cao, J., Ploss, A., Rice, C.M., Xiang, Y., 2012. C7L family of poxvirus host range genes inhibits antiviral activities induced by type I interferons and interferon regulatory factor 1. J. Virol. 86, 4538–4547.
Nakazawa, Y., Emerson, G.L., Carroll, D.S., Zhao, H., Li, Y., Reynolds, M.G., Karem, K.L., Olson, V.A., Lash, R.R., Davidson, W.B., Smith, S.K., Levine, R.S., Regnery, R.L., Sammons, S.A., Frace, M.A., Mutasim, E.M., Karsani, M.E., Muntasir, M.O., Babiker, A.A., Opoka, L., Chowdhary, V., Damon, I.K., 2013. Phylogenetic and ecologic perspectives of a monkeypox outbreak, southern Sudan, 2005. Emerg. Infect. Dis. 19, 237–245.
Next Advance, 2012. Protocols for BBX24 Models. Next Advance, Averill Park, NY.
Ng, A., Tscharke, D.C., Reading, P.C., Smith, G.L., 2001. The vaccinia virus A41L protein is a soluble 30 kDa glycoprotein that affects virus virulence. J. Gen. Virol. 82, 2095–2105.
Osorio, J.E., Iams, K.P., Meteyer, C.U., Rocke, T.E., 2009. Comparison of monkeypox viruses pathogenesis in mice by *in vivo* imaging. PloS One 4, e6592.
Pires de Miranda, M., Reading, P.C., Tscharke, D.C., Murphy, B.J., Smith, G.L., 2003. The vaccinia virus kelch-like protein C2L affects calcium-independent adhesion to the extracellular matrix and inflammation in a murine intradermal model. J. Gen. Virol. 84, 2459–2471.
Price, N., Tscharke, D.C., Hollinshead, M., Smith, G.L., 2000. Vaccinia virus gene B7R encodes an 18- kDa protein that is resident in the endoplasmic reticulum and affects virus virulence. Virology 267, 65–79.
Price, N., Tscharke, D.C., Smith, G.L., 2002. The vaccinia virus B9R protein is a 6 kDa intracellular protein that is non-essential for virus replication and virulence. J. Gen. Virol. 83, 873–878.
Reynolds, M.G., Damon, I.K., 2012. Outbreaks of human monkeypox after cessation of smallpox vaccination. Trends Microbiol. 20, 80–87.
Rimoin, A.W., Mulembakani, P.M., Johnston, S.C., Lloyd Smith, J.O., Kisalu, N.K., Kinkela, T.L., Blumberg, S., Thomassen, H.A., Pike, B.L., Fair, J.N., Wolfe, N.D., Shongo, R.L., Graham, B.S., Formenty, P., Okitolonda, E., Hensley, L.E., Meyer, H., Wright, L.L., Muyembe, J.J., 2010. Major increase in human monkeypox incidence 30 years after smallpox vaccination campaigns cease in the Democratic Republic of Congo. Proc. Natl. Acad. Sci. USA 107, 16262–16267.
Santos, C.R., Blanco, S., Sevilla, A., Lazo, P.A., 2006. Vaccinia virus B1R kinase interacts with JIP1 and modulates c-Jun-dependent signaling. J. Virol. 80, 7667–7675.
Seet, B.T., Johnston, J.B., Brunetti, C.R., Barrett, J.W., Everett, H., Cameron, C., Sypula, J., Nazarian, S.H., Lucas, A., McFadden, G., 2003. Poxviruses and immune evasion. Ann. Rev. Immunol. 21, 377–423.
Senkevich, T.G., Koonin, E.V., Buller, R.M., 1994. A poxvirus protein with a RING zinc finger motif is of crucial importance for virulence. Virology 198, 118–128.
Shchelkunov, S.N., Totmenin, A.V., Babkin, I.V., Safronov, P.F., Ryazankina, O.I., Petrov, N.A., Gutorov, V.V., Uvarova, E.A., Mikheev, M.V., Sisler, J.R., Esposito, J.J., Jahrling, P.B., Moss, B., Sandakhchiev, L.S., 2001. Human monkeypox and smallpox viruses: genomic comparison. FEBS Lett. 509, 66–70.
Shisler, J.L., Jin, X.L., 2004. The vaccinia virus K1L gene product inhibits host NF-kappaB activation by preventing IkappaBalpha degradation. J. Virol. 78, 3553–3560.
Tamin, A., Esposito, J., Hruby, D., 1991. A single nucleotide substitution in the 5′-untranslated region of the vaccinia N2L gene is responsible for both alpha-amanitin-resistant and temperature-sensitive phenotypes. Virology 182, 393–396.
Verardi, P.H., Jones, L.A., Aziz, F.H., Ahmad, S., Yilma, T.D., 2001. Vaccinia virus vectors with an inactivated gamma interferon receptor homolog gene (B8R) are attenuated *In vivo* without a concomitant reduction in immunogenicity. J. Virol. 75, 11–18.
Weaver, J.R., Isaacs, S.N., 2008. Monkeypox virus and insights into its immunomodulatory proteins. Immunol. Rev. 225, 96–113.
Xia, X., 2013. DAMBE5: a comprehensive software package for data analysis in molecular biology and evolution. Mol. Biol. Evol. 30, 1720–1728.